PREDICTING GROUND-BASED AEROSOL OPTICAL DEPTH WITH SATELLITE IMAGES VIA GAUSSIAN PROCESSES

Goo Jun, Joydeep Ghosh
Department of Electrical and Computer Engineering, University of Texas, Austin, TX, U.S.A.

Vladan Radosavljevic, Zoran Obradovic
Information Science and Technology Center, Temple University, Philadelphia, PA, U.S.A.

Keywords: Aerosol, AERONET, MODIS, Gaussian Process, Active Learning, Spatio-temporal Data Mining.

Abstract: A Gaussian process regression technique is proposed to predict ground-based aerosol optical depth measurements from satellite multispectral images, and to select the most informative ground-based sites by active learning. Satellite images provide spatial and temporal information in addition to the spectral features, and such heterogeneity of available features is captured in the Gaussian process model by employing an additive set of covariance functions. By finding an optimal set of hyperparameters, relevance of each additional information is automatically determined. Experiments show that the spatio-temporal information contributes significantly to the regression results. The prediction results are not only more accurate but also more interpretable than existing approaches. For active learning, each spatio-temporal setup is evaluated by an uncertainty-sampling algorithm. The results show that the active selection process benefits most from the spatial information.

1 INTRODUCTION

Aerosols are microscopic particles or liquid drops that are suspended in the Earth's atmosphere, and have significant effects on human health (Baron, 2006) and climate changes (Solomon et al., 2007). Aerosols are produced by natural and man-made sources and both reflect and absorb incoming solar radiation. One of the biggest challenges of current climate research is to characterize large spatial and temporal variations of aerosol concentrations, compositions, and sizes, which requires an integrated approach that effectively combines various types of measurements and modeling strategies. One way to quantitatively measure aerosol concentration is estimating the amount of sunlight absorbed by aerosols, which is called the aerosol optical depth (AOD) (Dubovik and King, 2000).

There are two major types of instruments whose measurements can provide info about AOD:
1) Ground instruments, represented by Aerosol Robotic Network (AERONET) is a global network of about 250 operational radiometers (Holben et al., 1998). AERONET provides more accurate measurements with higher temporal resolution compared to the satellite-based observations, but the data is available only from a limited number of sites at fixed locations.
2) Satellite instruments, such as Moderate Resolution Imaging Spectroradiometer (MODIS).MODIS is a multispectral sensing instrument in NASA's Terra and Aqua satellites (King and Kaufman, 1992). The MODIS data covers the entire Earth's surface on a daily basis, but is usually less accurate than the ground-based information.

Most operational aerosol prediction algorithms are deterministic, constructed as inverse operators of high-dimensional non-linear functions according to the domain knowledge (Remer et al., 2006). As an alternative, a novel statistical approach of training a nonlinear regression model using the satellite observations as inputs and ground based measurements as targets was suggested in (Han et al., 2006). It has been shown that such a statistical approach could improve the accuracy of predictions significantly as compared to the operational domain-based methods.

The statistical model proposed in this paper has two objectives: one is making better and more interpretable AOD retrievals for locations without ground sensors, and the other is assisting the placements of ground-based sensors to obtain more informative groundtruth. The first objective is addressed by adopt-

Jun G., Ghosh J., Radosavljevic V. and Obradovic Z..
PREDICTING GROUND-BASED AEROSOL OPTICAL DEPTH WITH SATELLITE IMAGES VIA GAUSSIAN PROCESSES.
DOI: 10.5220/0003115203700375
In *Proceedings of the International Conference on Knowledge Discovery and Information Retrieval* (KDIR-2010), pages 370-375
ISBN: 978-989-8425-28-7

ing a Gaussian process (GP) regression model that can easily incorporate auxiliary information such as spatial and temporal information from the satellite measurements. Importances and sensitivities of these features are automatically determined by tuning hyperparameters of covariance functions. The second is objective is addressed by employing an active learning algorithm to select the most informative sites from a fixed set of candidate locations. Uncertainty scores for active learning can be easily approximated by the predictive variances of the fitted Gaussian process. In this study we are interested in prediction of AODs although the proposed methods are applicable to a larger class of remote sensing problems.

2 RELATED WORK

Non-linear regression models in data-driven prediction of atmospheric properties were discussed in (Müller et al., 2003). Statistical methods for the prediction of AOD at a global scale from integrated ground and satellite-based data were proposed in (Han et al., 2006), where neural networks trained on satellite observations spatially-temporally merged with AERONET measurements were used to predict AOD. This approach achieved higher prediction accuracy than the currently used operational knowledge-based algorithm (Han et al., 2005), and could aid domain scientists in understanding sources of correctable prediction errors (Vucetic et al., 2008).

A neural network-based regression algorithm was proposed for AOD retrieval by Radosavljevic *et al* (Radosavljevic et al., 2009). The authors also considered a scenario that a number of AERONET sites are removed from operation, and proposed a method to maintain the most informative sites. The proposed goodness criterion for the selection was how close the accuracy of a regression model built on data from a reduced sensor set was to the accuracy of a model built of the entire set of sensors. This approach does not utilize spatial nor temporal information in regression, though. An active learning algorithm has been proposed by Das *et al* (Das et al., 2009), where an ensemble of neural networks are constructed by bootstrapping. In this work, spatial and temporal diversities are used in the active selection process, but not included in the prediction model, either.

The proposed method exploits spatio-temporal correlation between instances using GP regression. Statistical modeling of spatially varying data has long been studied as an important field of statistics, called spatial statistics or geostatistics. Kriging is a well-known technique to model spatial dependencies of data, and it has been widely applied to various problems of spatial statistics (Cressie, 1993). The kriging approach has recently been adopted by the machine learning community, where it is referred to as a Gaussian process model (Rasmussen and Williams, 2005). The next section summarizes the key features of this model.

3 GAUSSIAN PROCESSES

A jointly Gaussian random vector $\mathbf{x} = [x_1, x_2, x_3, ...x_n]^T$ is denoted as $\mathbf{x} \sim \mathcal{N}(\mu, \Sigma)$, where μ is the mean vector and Σ is the covariance matrix. One useful property of a Gaussian random vector is that conditional and marginal distributions of Gaussian random vectors are also Gaussian. A Gaussian process is a random process such that all finite dimensional distributions of the process are jointly Gaussian random vectors (Rasmussen and Williams, 2005).

Let x be a random process indexed by $\mathbf{s}$, then $x(\mathbf{s})$ is a Gaussian process if and only if $\mathbf{x} = [x(\mathbf{s}_1), x(\mathbf{s}_2), ..., x(\mathbf{s}_n)]^T$ is a jointly Gaussian random vector for any finite set of $S = \{\mathbf{s}_1, \mathbf{s}_2, ..., \mathbf{s}_n\}$. As a Gaussian distribution is defined by its mean and covariance, a Gaussian process is fully defined by a mean function $\mu(\mathbf{s})$ and a covariance function $k(\mathbf{s}_1, \mathbf{s}_2)$, and denoted as $x(\mathbf{s}) \sim \mathcal{GP}(\mu(\mathbf{s}), k(\mathbf{s}_1, \mathbf{s}_2))$. In Gaussian process regression (GPR), the target variable is modeled by a Gaussian random process. Let us assume that values of x are observed for some $S = \{\mathbf{s}_1, \mathbf{s}_2, ..., \mathbf{s}_n\}$, and $x(\mathbf{s})$ is modeled as $x(\mathbf{s}) = f(\mathbf{s}) + \varepsilon$, where ε is an additive white Gaussian noise term, $\varepsilon \sim \mathcal{N}(0, \sigma_\varepsilon^2)$. We assume a (zero-mean) Gaussian process prior for $f(\mathbf{s})$:

$$f(\mathbf{s}) \sim \mathcal{GP}(\mu(\mathbf{s}) = 0,\ k(\mathbf{s}_1, \mathbf{s}_2)) \ .$$

In regression problems, we are interested in making predictions based on the training data $\mathbf{x} = [x_1(\mathbf{s}_1), ..., x_n(\mathbf{s}_n)]^T$. The predictive distribution of an out-of-sample instance $x_*(\mathbf{s}_*)$ can be easily derived from the conditional distribution of jointly Gaussian random vectors, and is also Gaussian: $x_*(\mathbf{s}_*) \sim \mathcal{N}(\mu_*(\mathbf{s}_*), \sigma^2(\mathbf{s}_*))$:

$$\mu_*(\mathbf{s}_*) = \mathbf{k}(\mathbf{s}_*, S)[K_{SS} + \sigma_\varepsilon^2 I]^{-1}\mathbf{x} \ ,$$
$$\sigma^2(\mathbf{s}_*) = k(\mathbf{s}_*, \mathbf{s}_*) + \sigma_\varepsilon^2 - \mathbf{k}(\mathbf{s}_*, S)[K_{SS} + \sigma_\varepsilon^2 I]^{-1}\mathbf{k}(S, \mathbf{s}_*) \ ,$$

where $\mathbf{k}(\mathbf{s}_*, S) = [k(\mathbf{s}_*, \mathbf{s}_1), k(\mathbf{s}_*, \mathbf{s}_2), ..., k(\mathbf{s}_*, \mathbf{s}_n)]$, $\mathbf{k}(S, \mathbf{s}_*) = \mathbf{k}(\mathbf{s}_*, S)^T$, and K_{SS} is a matrix such that its (i, j)-th element $K_{ij} = k(\mathbf{s}_i, \mathbf{s}_j)$. As can be seen in the formula, the covariance function $k(\mathbf{s}_1, \mathbf{s}_2)$ fully determines the characteristics of a Gaussian process.

Table 1: List of features from MODIS data.

Feature	Description
$\mathbf{m}_i$	Average spectral responses (4-dim)
σ_i	Standard deviations (4-dim)
$\mathbf{a}_i$	Measurement angles (4-dim)
$\mathbf{t}_i$	Temporal information (d_i, h_i)
$\mathbf{s}_i$	Longitude and latitude (ϕ, θ)

4 METHODS

Gaussian process regressions are used to predict the AERONET AOD values from the spatio-temporally collocated MODIS data. Table 1 shows the 16 features available from the MODIS data.

Since we have heterogeneous features, using a single covariance function with the Euclidean distance measure is not appropriate. Instead, each subset of features is modeled using a separate covariance function designed just for the features. First, isometric squared exponential covariance functions are used for the baseline features.

$$k_1(\mathbf{m}_i, \mathbf{m}_j) = v_1^2 \exp\left(-\frac{||\mathbf{m}_i - \mathbf{m}_j||^2}{2\lambda_m^2}\right),$$

$$k_2(\mathbf{a}_i, \mathbf{a}_j) = v_2^2 \exp\left(-\frac{||\mathbf{a}_i - \mathbf{a}_j||^2}{2\lambda_a^2}\right).$$

There are two different features in the temporal information $\mathbf{t}_i = (d_i, h_i)$, where d_i indicates day of the year and h_i is the time of the day in minutes. Since d_i and h_i could have different roles in the prediction of aerosol depths, a non-isometric covariance function is employed to allow different length scales:

$$k_3(\mathbf{t}_i, \mathbf{t}_j) = v_3^2 \exp\left(-\frac{\Delta_d(d_i, d_j)^2}{2\lambda_d^2} - \frac{\Delta_h(h_i, h_j)^2}{2\lambda_h^2}\right).$$

Because of the periodic nature of temporal features, distances Δ_d and Δ_h are adjusted for properly interpretation of the actual temporal differences:

In case of spatial information, $\mathbf{s}_i = (\phi_i, \theta_i)$ is a coordinate in the spherical coordinate system. The Euclidean distance is not a correct distance measure for our problem, since we want the geodesic distance along the surface of the earth. The geodesic distance on the surface of a sphere is usually referred to as the great-circle distance. The haversine formula is used to approximate the angular distance (Sinnott, 1984). The great-circle distance is approximated as the arc length obtained from the angular distance: $R\Delta_s$, where R is the radius of the Earth. We do not consider R as a factor since it will be automatically incorporated in the length parameter, λ_s. The covariance function for the spatial information is hence modeled as:

$$k_4(\mathbf{s}_i, \mathbf{s}_j) = v_4^2 \exp\left(-\frac{\Delta_s(\mathbf{s}_i, \mathbf{s}_j)^2}{2\lambda_s^2}\right).$$

It is also possible to treat longitude and latitude data separately instead of using the great circle distance, since the measurements could be more affected from the longitude information than from the latitudes. We tried the setup also, but did not get good results. It also appears that the hyperparameters for longitude and latitude covariance functions are not much different, which means that there is not much advantage in the separation approach.

The spatial covariance matrix is not positive definite, because we have multiple instances of data collected from each location. Many $\mathbf{s}_i$'s have the exactly same value; hence the resulting covariance matrix has identical rows and columns. Since a positive definite covariance matrix is required for GPR, we add small perturbations to the values of $\mathbf{s}_i$, proportional to the measurement noise. In Table 1, σ_i is a feature that indicates the standard deviations in the measured spectrum. We used the averaged standard deviation, $\bar{\sigma}_i$, to add random noise to the spatial features:

$$\phi_i = \phi_i + N(0, \bar{\sigma}_i) \ , \quad \theta_i = \theta_i + N(0, \bar{\sigma}_i) \ .$$

The overall covariance function is obtained by simply adding the aforementioned covariance functions, as a sum of positive definite kernels is also a positive definite kernel (Rasmussen and Williams, 2005). We consider four different settings in this paper. $k_\varepsilon = v_\varepsilon^2 \delta_{ij}$ is a term for noise, where δ_{ij} is a kronecker-delta function:

1. Baseline: $k = k_1 + k_2 + k_\varepsilon$.
2. Temporal: $k = k_1 + k_2 + k_3 + k_\varepsilon$.
3. Spatial: $k = k_1 + k_2 + k_4 + k_\varepsilon$.
4. Spatio-temporal: $k = k_1 + k_2 + k_3 + k_4 + k_\varepsilon$.

Once the covariance function is designed, the next step is selecting the hyperparameters. The most complicated model is the spatio-temporal model, which has ten hyperparameters. Hyperparemeters are selected by minimizing the negative log likelihood by the gradient descent method. To avoid local minima and for faster search, a randomized algorithm is used by selecting a random subset of samples from the training data. Each randomized search result is then evaluated using the entire training data, and the set of hyperparameters with the highest log-likelihood score is selected.

An uncertainty sampling approach (Lewis and Gale, 1994) is used to perform active learning. In contrast to loss-reduction methods, uncertainty sampling generally does not require the model to be re-trained for every unlabeled instance. Instead, each instance in the unlabeled dataset is assigned an uncertainty score predicted by the model trained on the labeled data. In the Gaussian process model, there is a natural measure of uncertainty, the posterior variance $\sigma^2(\mathbf{s}_*)$. The

predictive distribution of the model provides the variance of an out-of sample instance as well as the mean. At each stage of the active learning process, we simply select the site that has the highest average variance.

5 EXPERIMENTS

GP Regression. Datasets for experiments were created by collecting spatio-temporally MODIS and AERONET measurement data over 70 AERONET sites for years 2005 and 2006. The 2005 data is subsampled to construct 10 randomly selected training sets, where each set contains data from 30 AERONET sites. We used the same set of training datasets as used in (Radosavljevic et al., 2009) to make the results comparable; hence please refer to the paper for details on the data preparation. Baseline, temporal, spatial, and spatio-temporal GP models are trained with each training set, and tested on the test data from 2006. In previous studies, it was observed that the variance of the AERONET AOD data increases as the AOD value increases, and using square-root values of the target variable helps making better predictions. We use the same approach, and R^2 scores are calculated by first squaring the predicted values and comparing them to the original AOD values. 10 sets of 300 randomly selected samples are used for hyperparameter optimization.

Table 2 shows the R^2 scores obtained from the four proposed settings, as well as the current state-of-the-art approach using an ensemble of neural nets (Radosavljevic et al., 2009). The spatio-temporal model shows better results than the baseline results in a statistically significant manner, and the spatial information appears to be more informative than the temporal information. Table 3 shows the estimated hyperparameters $(v_1^2, \ldots v_4^2, v_\varepsilon^2)$ that determine how much each covariance function contributes to the predicted value. Hyperparameters are estimated using one of the training datasets. As shown in the table, the spectral features are the most dominant features, and the measurement angles second. The spatial information has smaller significance, but is much more relevant than the temporal information. Table 4 shows the estimated length parameters $(\lambda_m, \lambda_a, \lambda_d, \lambda_t, \lambda_s)$ using the same training set, indicating that the degree of correlation associated with each feature. Since different features have different physical dimensions, units of each length scale are shown in the table. It is noticeable that the time of the day has very short length parameter, λ_t, meaning that the prediction depends on the time features only if the time difference between the test and the training instances is very small.

Table 2: R^2 scores with baseline, temporal, spatial, and spatio-temporal features, and using neural networks.

	Basel.	Temporal	Spatial	Spatio-temp.	NN*
Mean	0.7160	0.7376	0.7622	**0.7726**	0.746
Median	0.7208	0.7401	0.7706	**0.7748**	0.754
Std. Dev.	0.0162	0.0243	0.0263	0.0180	0.042

*(Radosavljevic et al., 2009)

Table 3: Variance parameter associated with each covariance function.

	Baseline	Temporal	Spatial	Spatio-temp.
v_1^2 (spectral)	1.560	2.8123	1.1548	1.528
v_2^2 (angle)	0.5471	1.6525	0.6615	0.8122
v_3^2 (temporal)	-	0.00450	-	0.00190
v_4^2 (spatial)	-	-	0.00876	0.0112
v_ε^2 (noise)	-	0.00638	0.00613	0.00718

Active Learning. For active learning experiments, five sites are randomly selected to construct the initial training data. One site is added to the training data after each active learning step. Each site in 2005 data has 70 instances, and the uncertainty score for each site is the average over all 70 instances. Each experimented is repeated 10 times. To save computational time, five sets of 200 randomly selected samples are used to optimize hyperparameters. Using fewer samples resulted in slightly lower R^2 scores for the same number of randomly selected sites compared to the results in the previous section.

Fig. 1 shows the learning curves from temporal and spatial methods, and each method is tested using passive (random) and active learning algorithms. The spatial results show significant improvements by using active learning algorithms, but not the temporal results. A plausible explanation is that the use of the temporal kernel yields high variances on the instances having longer temporal distances, but having temporally distant measurements in 2005 do not guarantee the same informational gain for the 2006 data. In contrast, spatial distances remain the same both in the training and the test data. Fig. 2(a) shows the active learning results for four GP setups. It is clear that temporal information adds valuable information for

Table 4: Length parameter associated with each covariance function.

	Baseline	Temporal	Spatial	Spatio-temp.
λ_m (normalized)	0.2136	0.3031	0.1704	0.3441
λ_a (degree)	86.91	105.4	101.2	121.7
λ_d (days)	-	17.23	-	14.75
λ_t (minutes)	-	0.2958	-	0.1267
λ_s (radian)	-	-	0.1348	0.1491

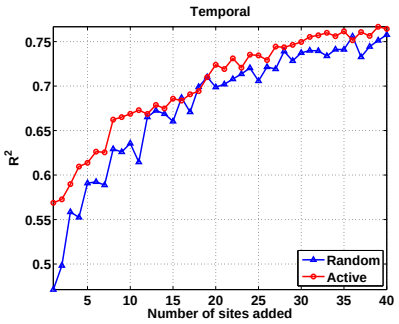

(a) Temporal

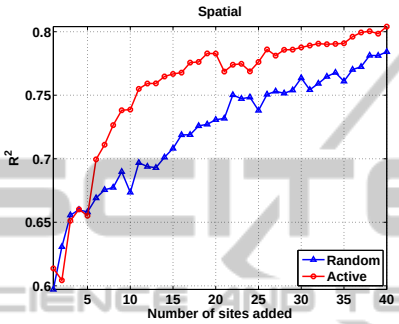

(b) Spatial

Figure 1: R^2 scores from passive and active learning algorithms with different features.

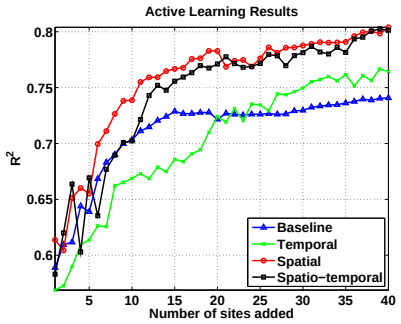

(a) Active learning results

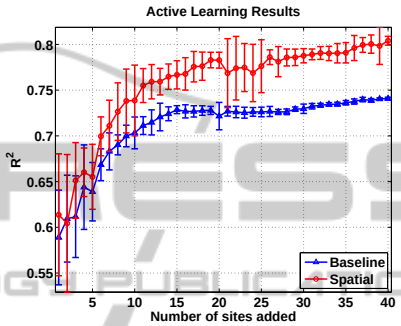

(b) Baseline *vs.* spatial

Figure 2: Active learning results. (a) results from four different settings. Error bars are removed for visibility (b) spatial active learning compared to the base line with error bars of one standard deviation.

making predictions, but not for active learning, compared to the spatial information. The best (spatial) and the worst (baseline) learning curves with error bars of one standard deviation are presented in Fig. 2(b) to show statistical significance of results. Fig. 3 shows the locations of 30 actively selected sites on the world maps. All experiments are started with the same initial training set, marked with red squares. 30 actively selected sites are shown with numbers that indicates the order of selection. It is observable that the baseline result has regions with densely located sites, while the spatial one has more dispersed selections.

6 CONCLUSIONS

Gaussian process regressions are used to predict ground-based aerosol optical depth measurements with satellite-taken multispectral images. Heterogeneous features with spatial and temporal information are incorporated together by employing a set of covariance functions, and it is shown that the spatio-temporal information adds valuable information to the regression model. An uncertainty-sampling based active learning algorithm is tested with each regression setup. It turns out that the active selection process

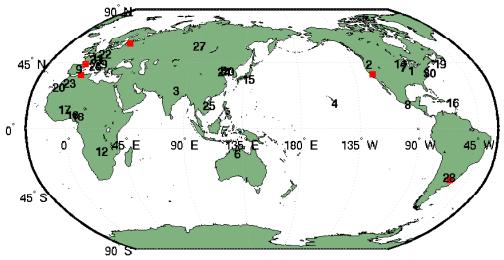

(a) Baseline

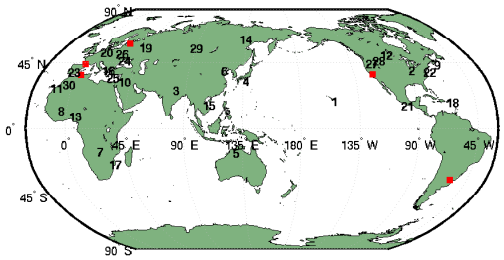

(b) Spatial

Figure 3: Sites picked by active learning with four different settings. Red squares are five sites included in the initial training set, and numbers indicate the order of selection by active learning.

benefits most by adding spatial information compared to the baseline method. As a possible extension to the proposed method, the square-root transform of the dependent variable can be incorporated into the Gaussian process model, but this idea requires further studies since it involves designing a non-stationary covariance function.

ACKNOWLEDGEMENTS

This work was supported by NSF Grants IIS-0705815 and IIS-0612149.

REFERENCES

Baron, P. (2006). Generation and Behavior of Airborne Particles (Aerosols). *National Institute of Occupational Health and Safety, http://www. cdc. gov/niosh/topics/aerosols/pdfs/Aerosol_101. pdf. Retrieved on June*.

Cressie, N. (1993). *Statistics for Spatial Data*. Wiley, New York.

Das, D., Obradovic, Z., and Vucetic, S. (2009). Active selection of sensor sites in remote sensing applications. In *IEEE International Conference on Data Mining (ICDM 09)*.

Dubovik, O. and King, M. (2000). A flexible inversion algorithm for retrieval of aerosol optical properties from Sun and sky radiance measurements. *Journal of Geophysical Research*, 105(D16):20676.

Han, B., Obradovic, Z., Li, Z., and Vucetic, S. (2006). Data Mining Support for the Improvement of MODIS Aerosol Retrievals. In *IEEE International Conference on Geoscience and Remote Sensing Symposium, 2006. IGARSS 2006*, pages 2453–2456.

Han, B., Vucetic, S., Braverman, A., and Obradovic, Z. (2005). Construction of a geospatial predictor by fusion of global and local models. In *Proccedings of 8th International Conference on Information Fusion*. Citeseer.

Holben, B., Eck, T., Slutsker, I., Tanre, D., Buis, J., Setzer, A., Vermote, E., Reagan, J., Kaufman, Y., Nakajima, T., et al. (1998). AERONET–A federated instrument network and data archive for aerosol characterization. *Remote Sensing of Environment*, 66(1):1–16.

Kaufman, Y., Tanré, D., Remer, L., Vermote, E., Chu, A., and Holben, B. (1997). Operational remote sensing of tropospheric aerosol over land from EOS moderate resolution imaging spectroradiometer. *J. Geophys. Res*, 102(17):051–17.

King, M. and Kaufman, J. (1992). Remote sensing of cloud, aerosol, and water vapor properties from the Moderate Resolution Imaging Spectrometer (MODIS). *IEEE Transactions on Geoscience and Remote Sensing*, 30(1).

Lewis, D. D. and Gale, W. A. (1994). A sequential algorithm for training text classifiers. In *Proceedings of the 17th Annual International ACM SIGIR Conference on Research and Development in Information Retrieval*, pages 3–12. Springer-Verlag New York, Inc.

Müller, M., Kaifel, A., Weber, M., Tellmann, S., Burrows, J., and Loyola, D. (2003). Ozone profile retrieval from Global Ozone Monitoring Experiment (GOME) data using a neural network approach (neural network ozone retrieval system (NNORSY)). *J. Geophys. Res*, 108(D16):4497.

NASA (retrieved in 2010). *Official MODIS website, http://modis.gsfc.nasa.gov/*.

Radosavljevic, V., Vucetic, S., and Obradovic, Z. (2009). Reduction of ground-based sensor sites for spatio-temporal analysis of aerosols. In *SensorKDD '09: Proceedings of the Third International Workshop on Knowledge Discovery from Sensor Data*, pages 71–78, New York, NY, USA. ACM.

Rasmussen, C. (1996). *Evaluation of Gaussian processes and other methods for non-linear regression*. PhD thesis, University of Toronto.

Rasmussen, C. E. and Williams, C. K. I. (2005). *Gaussian Processes for Machine Learning*. The MIT Press.

Remer, L., Tanré, D., Kaufman, Y., Levy, R., and Mattoo, S. (2006). Algorithm for remote sensing of tropospheric aerosol from MODIS: Collection 005. *modis. gsfc. nasa. gov/data/atbd/atbd_mod02. pdf*.

Seung, H. S., Opper, M., and Sompolinsky, H. (1992). Query by committee. In *Proceedings of the Fifth Annual Workshop on Computational Learning Theory*, pages 287–294, Pittsburgh, PA, USA. ACM Press.

Sinnott, R. (1984). Virtues of the Haversine. *Sky and telescope*, 68:158.

Solomon, S., Qin, D., Manning, M., Chen, Z., Marquis, M., Averyt, K., Tignor, M., and Miller, H. (2007). IPCC 2007. Climate Change 2007: the Physical Science Basis Contribution of Working Group I to the Fourth Assessment Report of the Intergovernmental Panel on Climate Change.

Vucetic, S., Han, B., Mi, W., Li, Z., and Obradovic, Z. (2008). A Data-Mining Approach for the Validation of Aerosol Retrievals. *IEEE Geoscience and Remote Sensing Letters*, 5(1):113–117.